Analysis of thermophysical parameters of solar water desalination plant with an external camera

N Rakhimov[1*], *Kh* Akhmadov[2], *A* Komilov[2], *K* Rashidov[2], and *L* Aliyarova[1]

[1]Karshi Engineering Economics Institute, Karshi, 180100, Uzbekistan
[2]Physical-Technical Institute of the Academy of Sciences of the Republic of Uzbekistan, Tashkent, Uzbekistan

Abstract. In this work, an analysis of the thermophysical processes taking place inside a specially designed chamber with a geometry different from other works was carried out. This process is designed in COMSOL Multiphysics software. Boundary conditions were investigated for ambient temperature of 293.15 K and solar radiation of 1000 W/m^2. The process was taken as natural convection. In this case, the flow of air with high humidity inside the solar water heater was analyzed. It can be seen that the air temperature rises to 450 K. At the same time, the speed of moist air inside the chamber, heat flow and other thermophysical quantities were determined and analyzed.

1 Introduction

The growing industrialization, particularly in developing nations, coupled with a heightened concern for environmental preservation, has led to an escalated desire for clean and environmentally friendly renewable energy sources. This demand specifically includes wind and solar energy, aimed at generating both freshwater and electricity [1]. Solar energy can meet the energy needs of the world using a few percent of uninhabited areas [1-5]. In a prior study, it was found that around 40% of the global energy production is dedicated to heating purposes [5]. At the same time, despite the fact that 97% of the Earth's surface is covered with water, most of the water is located in the oceans and seas, which are considered unsuitable for drinking. The increasing pollution of surface and underground water from year to year shows that this problem is more urgent. Based on the above, desalination of salt water is important in solving the problem of drinking water. The industrial application of salt water desalination technology began in the 1950s [6]. However, the high energy consumption of desalination, the large amount of greenhouse gases, the increase in the amount of salt waste, and the high operating costs prevented this technology from being widely adopted [7]. Currently, the use of renewable energy is an effective way to solve this problem. Among them, solar energy is clean, harmless, available in any region and stable[8,9]. At present, a large number of research works have been carried out to improve the efficiency of solar water purifiers. For example, in AE et al. [10], the methods of improving the design of horizontal and vertical solar water purifiers are

* Corresponding author: rahimov1570@gmail.com

considered. According to it, it was determined that the price of water for one kilogram in tubular solar water dispensers is between 0.0061 and 0.2 US dollars. Mariem et al. [11] only studied the geometrical dimensions of solar water desalinations, the wick material. Swellam et al. [12] conducted a study on thermal analysis and device performance improvement on a tubular solar water heater. Arunkumar et al. [13] only studied and classified solar water heaters with efficiencies greater than 5 L/m^2 and also considered the heat transfer mechanism in the devices. Hemant et al [14] analyzed different sloped solar stills and found that active sloped solar stills have the highest efficiency for fresh water. Inspired by the work analyzed above, CFD analysis of the solar water desalination device was found to be appropriate.

2 Methods and materials

The initial phase in conducting a Computational Fluid Dynamics (CFD) analysis for any issue involves developing a geometric model that aligns with the design specifications. In this context, the designated problem domain encompasses the area enclosed by the surface of the saltwater within the still basin, the surrounding side walls, the front and back boundaries, and the transparent cover of the solar still. A schematic view of the solar water purifier is shown in Figure 1. The dimensions of the main camera are width-1 m, depth-1 m, height-0.9 m. The section where salt water is poured consists of width-1 m, depth-1 m, height-0.1 m. A separate section connected to the main chamber is a chimney and its height is 2 m. The 3D geometry of the two-chamber solar water heater was created in COMSOL Multiphysics software, and Figure 1 shows the schematic model of the designed 3D model.

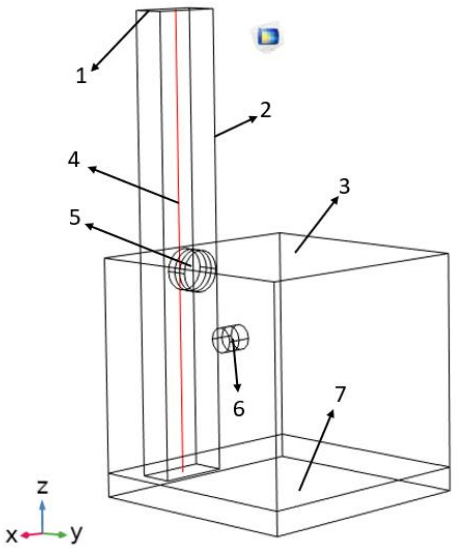

Fig. 1. Schematic view of the solar water desalination. 1- chamber for the exit of moist air, 2-separate compartment, 3- the main transparent-walled camera, 4-Cut Line 3D for results, 5- hole connecting the main chamber and the chamber, 6- hole for incoming air flow from the outside, 7- section with salt water poured under the active element [15].

Establishing accurate boundary conditions and their types played a crucial role in achieving precise solutions for fluid flow problems [16-22]. While certain boundary conditions were determined based on physical phenomena, others were set using the simulation software COMSOL Multiphysics. table 1 provides a comprehensive overview of

the boundary conditions and types assigned to various segments within the analyzed domain.

Table 1. The thermophysical properties of materials and boundary condition.

Fluid	**Gas**	**Property**	**Boundary condition**		
Water	**Air**		**Ambient temperature**	**Solar radiation**	**Acceleration gravity**
4200 1000 0.6 210e-6 4.18	1000 1.29 0.027 0.0034 1.4	Heat capacity at constant pressure [J/(kg·K)] Density [kg/m³] Thermal conductivity [W/(m·K)] Coefficient of thermal expansion [1/K] Ratio of specific heats [kJ/(g·K)]	293.15 K	1000 W/m^2	9.71 m/s^2

Choosing appropriate boundary conditions is a crucial aspect of CFD simulation. Every CFD tool resolves the equations inherent in the modeling based on the constraints imposed by the specified boundary conditions. The actual or physical boundary conditions are conceptualized and simplified to incorporate them into the simulation. For example, in this investigation, the side walls of the solar water desalination, designed as insulated, were treated as adiabatic in the simulation. Three-dimensional numerical simulations were performed in the COMSOL Multiphysics program at laminar flow, turbulent flow, heat transfer in solid and fluids physics interfaces, and the FEM (finite element method) method was used for the solution. The boundary conditions in table 1 above were given and the following results were obtained.

3 Results and Discussion

COMSOL Multiphysics employs the finite element method, and in adherence to the software's Multiphysics concept, four interconnected “application modules” are employed to simulate the phenomenon of three-dimensional diffusive double convection. These modules address fluid flow, heat transfer, and mass transfer. Model was simulated with stationary state and boundary conditions are given in the table 1. Results were obtained according to Cut Line 3D see the Figure 1.

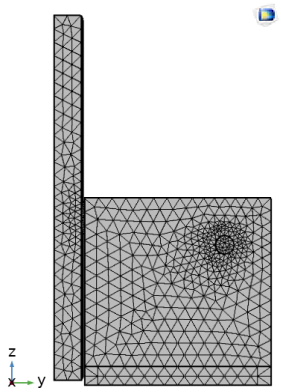

Fig. 2. Selected mesh for the model (FEM).

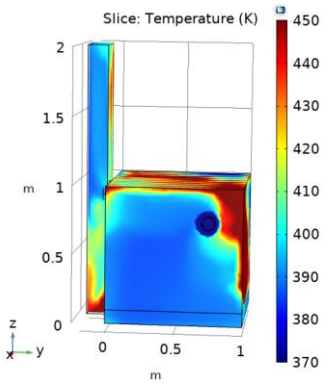

Fig. 3. Temperature distribution over the entire volume of the solar water desalination.

In Figure 2, the generated mesh is depicted. The choice of mesh applied to model geometry is crucial in influencing the model's resolution process. Additionally, from figure 3, it can be observed that the maximum surface temperature of the SWD (Solar Water Desalination) system reached approximately 450 K, while the minimum temperature was recorded at 370 K.

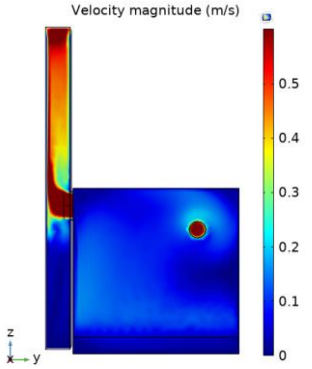

Fig. 4. Velocity distribution for water vapor over the entire volume of the solar water desalination.

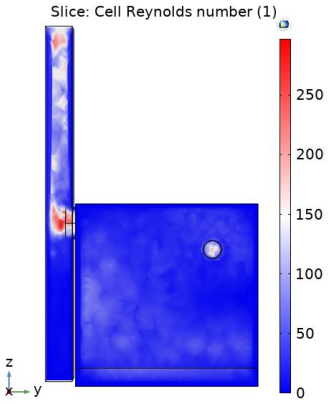

Fig. 5. Variation of the Reynolds number according to the volume of the solar water desalination.

Examining Figure 4 in detail, it illustrates the variation in air velocity within the SWD system, ranging from 0 m/s to 0.6 m/s in natural convection mode. Figure 5 presents the

variation of the Reynolds number in the SWD system. It was determined that the Reynolds number varied from 0-250.

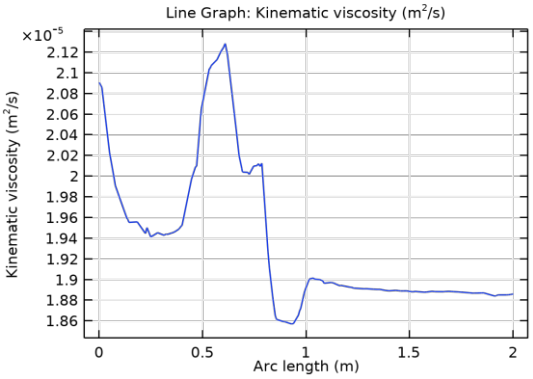

Fig. 6. 3D Cut Line Graph: Kinematic viscosity (m^2/s).

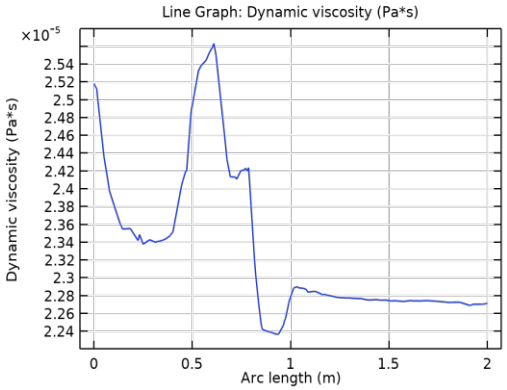

Fig. 7. 3D Cut Line Graph: Dynamic viscosity (Pa*s).

Figures 6-9 show the results obtained for the 4-Cut Line shown in figure 1. Kinematic viscosity of the air coming out through the chimney reaches from $1.86 \cdot 10^{-5}\ m^2/s$ minimum to $2.13 \cdot 10^{-5}\ m^2/s$ maximum (Figure 6). And in figure 7, Dynamic Viscosity is defined, we can see that it changes from $2.23 \cdot 10^{-5}\ Pa \cdot s$ to $2.57 \cdot 10^{-5}\ Pa \cdot s$.

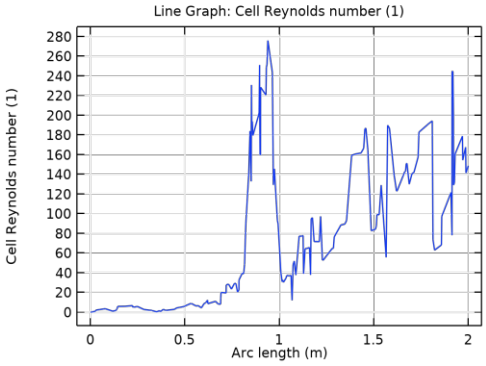

Fig. 8. 3D Cut Line Graph: Cell Reynolds number (1).

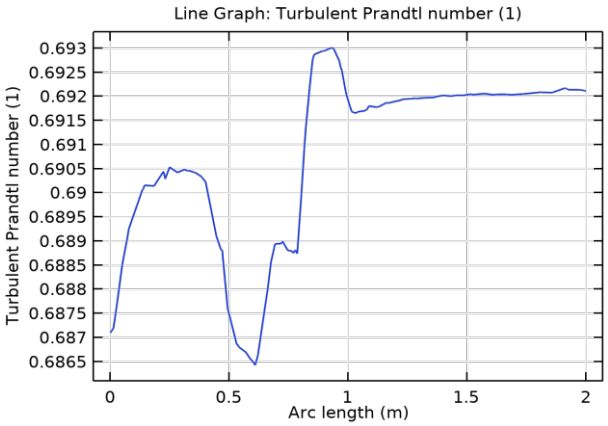

Fig. 9. 3D Cut Line Graph: Turbulent Prandtl number (1).

Figures 8 and 9 show the results of variation of Reynolds number and Prandtl number along the 3D Cut Line, where the Reynolds number varies from 0-280 along the 3D Cut Line. and the Prandtl number was found to vary from 0.6865 to 0.6930.

For Heat Transfer in Solids

Following equation is utilized for solving the Heat Transfer in Solids Interface.

$$\rho C_p\left(\frac{\partial \mathrm{T}}{\partial t}+\boldsymbol{u}_{trans}\cdot\nabla \mathrm{T}\right)+\nabla\cdot(\boldsymbol{q}+\boldsymbol{q}_r)=-\alpha \mathrm{T}:\frac{dS}{dt}+Q \tag{1}$$

$\rho$where, ρ is the density (kg/m^3), C_p is the specific heat capacity at constant stress (J/(kg·K)), T is the absolute temperature (K), u_{trans} is the velocity vector of translational motion (m/s), q is the heat flux by conduction (W/m^2), q_r is the heat flux by radiation (W/m^2), α is the coefficient of thermal expansion (1/K), S is the second Piola-Kirchhoff stress tensor (Pa), Q contains additional heat sources (W/m^3).

For Heat Transfer in Fluids

The Heat Transfer in Fluids Interface solves for the following equation

$$\rho \mathrm{Cp}\left(\frac{\partial \mathrm{T}}{\partial t}u\cdot\nabla \mathrm{T}\right)+\nabla\cdot(q+q_r)=\alpha_p \mathrm{T}\left(\frac{dp}{dt}+u\cdot\nabla_p\right)+\tau:\nabla u+Q \tag{2}$$

4 Conclusions

These analysis leads to following conclusion:

This study employs a 3-dimensional prototype to conduct thermal analysis of a solar water desalination system. The investigation encompasses variations in surface temperature, velocity magnitude, and absolute pressure within the system. Convective heat flux is manipulated across a range from 200 W/m² to 1000 W/m², with an observed concurrent increase in temperature, transitioning from 293.15 K to 450 K. Additionally, examination indicates that the outlet temperature of the freshwater vapor reaches approximately 400 K, considering an initial saltwater temperature of around 293.15 K. In natural mode, there is a slight change in velocity from 0 m/s to 0.6 m/s. Variation of Reynolds number and Prandtl number along the 3D Cut Line, where the Reynolds number varies from 0-280 along the 3D Cut Line. and the Prandtl number was found to vary from 0.6865 to 0.6930.

References

1. M. Alhashmi, G. Chhipi-shrestha, K.M. Nahiduzzaman, K. Hewage, R. Sadiq, Framework for developing a low-carbon energy demand in residential buildings using community-government partnership: An application in saudi arabia. Energies, **14**, 16, (2021)
2. J.S. Akhatov, K.S. Ahmadov, Extraction of Hydrogen from Water Using CeO<inf>2</inf> in a Solar Reactor Using a Concentrated Flux of Solar Radiation. Appl. Sol. Energy (English Transl. Geliotekhnika), **58**, 6 (2022)
3. S.A. Boltaev, K.S. Akhmadov, U.R. Gapparov, R. Djabbarganov, M.K. Kurbanov, D.S. Saidov, Thermotechnical and Adsorption Characteristics of the $SrCl_2$ Adsorbent for Ammonia Vapors in Solar Absorption Cycles. Appl. Sol. Energy, **58**, 1, 116–120, (2022)
4. J. Akhatov, K. Akhmadov, N. Juraboyev, Thermal performance enhancement in the receiver part of solar parabolic trough collectors. UNEC J. Eng. Appl. Sci., **3**, 2, 5–13 (2023)
5. N. Gunasekaran, Investigation on ETC solar water heater using twisted tape inserts. Mater. Today Proc., **47**, 5011–5016 (2021)
6. Z. Zhu, D. Peng, H. Wang, Seawater desalination in China: An overview. J. Water Reuse Desalin., **9**, 2, 115–132 (2019)
7. J. Liu, S. Chen, H. Wang, X. Chen, Calculation of Carbon Footprints for Water Diversion and Desalination Projects. Energy Procedia, **75**, 2483–2494 (2015)
8. A. Mollahosseini, A. Abdelrasoul, S. Sheibany, M. Amini, and S. K. Salestan, Renewable energy-driven desalination opportunities – A case study. J. Environ. Manage., **239**, 187–197 (2019)
9. G. Uzakov, S. Khamraev, S. Khuzhakulov, Rural house heat supply system based on solar energy. IOP Conf. Ser. Mater. Sci. Eng., **1030**, 1 (2021)
10. A.E. Kabeel, K. Harby, M. Abdelgaied, A. Eisa, A comprehensive review of tubular solar still designs, performance, and economic analysis. J. Clean. Prod., **246**, 119030 (2020)
11. M. Jobrane, A. Kopmeier, A. Kahn, H.M. Cauchie, A. Kharroubi, C. Penny, Internal and external improvements of wick type solar stills in different configurations for drinking water production– A review. Groundw. Sustain. Dev., **12**, 100519 (2021)
12. S.W. Sharshir, A.W. Kandeal, A.M. Algazzar, A. Eldesoukey, M.O.A. El-Samadony, A.A. Hussien, 4-E analysis of pyramid solar still augmented with external condenser, evacuated tubes, nanofluid and ultrasonic foggers: A comprehensive study. Process Saf. Environ. Prot., **164**, 408–417 (2022)
13. T. Arunkumar, A review of efficient high productivity solar stills. Renew. Sustain. Energy Rev., **101** (2018)
14. H.A. Kumar, Recent advancements, technologies, and developments in inclined solar still—a comprehensive review. Environ. Sci. Pollut. Res., **28**, **27**, 35346–35375 (2021)
15. Y.K. Rashidov, K.Y. Rashidov, I.I. Mukhin, K.T. Sur'atov, Z. Z. Rakhimov, Features of the Design of a Self-Draining Solar Power Plant with an Active Element. Appl. Sol. Energy (English Transl. Geliotekhnika), **54**, **3**, 178–182 (2018)
16. B. Toshmamatov, S. Shomuratova, S. Safarova, Improving the energy efficiency of a solar air heater with heat accumulator using flat reflectors. E3S Web of Conferences **411**, 01026 (2023)

17. B. Toshmamatov, *Modeling of thermal processes in a solar installation for thermal processing of municipal solid waste*, AIP Conference Proceedings, **2612**, 050027 (2023)
18. B. Sattorov, Kh. Davlonov, B. Toshmamatov, B. Arziev, *Increasing energy efficiency combined device solar dryer-water heater with heat accumulator*, BIO Web of Conferences, **71** 02024 (2023)
19. L.A. Aliyarova, U.H. Ibragimov, S.I. Khamraev, *Investigation of hydrodynamic processes in tubes of a combined solar collector*, AIP Conference Proceedings, 2612, 030018 (2023)
20. S.I. Khamraev, *Study of the combined solar heating system of residential houses*. BIO Web of Conferences, **71**, 02017 (2023)
21. Saydullo Khuzhakulov, Zokir Pardaev, Sardor Khamraev. *Thermal conditions of systems for solar thermal regeneration of adsorbents*. IPICSE 2020 IOP Conf. Series: Materials Science and Engineering, **1030**, 012166 (2021)
22. Sh. Mirzaev, J. Kodirov, S.I. Khamraev, *Method for determining the sizes of structural elements and semi-empirical formula of thermal characteristics of solar dryers*, APEC-V-2022, IOP Conf. Series: Earth and Environmental Science IOP Conf. Series: Earth and Environmental Science, **1070,** 012021 (2022)